CREEP DEFORMATIONS OF STRUCTURAL POLYMERIC MACROFIBERS

Rutger Vrijdaghs[(1)], Marco di Prisco [(2)] and Lucie Vandewalle [(1)]

[(1)] Department of Civil Engineering, KU Leuven, Belgium

[(2)] Department of Structural Engineering, Politecnico di Milano, Italy

Abstract

Fiber reinforced concrete (FRC) is a cementitious composite in which fibers are added to the fresh concrete to improve its behavior. Fibers can be added to bridge crack faces, thus increasing the residual load-bearing capacity of a concrete element. Furthermore, these fibers can arrest crack growth and increase the long-term durability of the structural element. However, long-term durability can be compromised by time-dependent phenomena such as creep. In FRC, time-dependent crack widening can be mainly attributed to two mechanisms: fiber creep and gradual fiber pull-out from the concrete matrix.

In the case of polymeric fibers, fiber creep in the crack may contribute significantly to the crack widening. This paper presents the experimental results of creep tests on two different commercially available polypropylene macrofibers. Different sustained load levels are considered, ranging from 22 % to 63 % of the fiber strength.

The results show that sudden failure occurs in the secondary creep phase at all load levels. Furthermore, the time to failure and the total strain at failure depend very strongly on the applied load level. The total creep strain at failure may become very large: creep coefficients greater than 10 have been observed, especially at lower load levels.

Keywords: fiber reinforcement, polymeric fiber, creep, experimental.

1. INTRODUCTION

Fiber reinforced concrete (FRC) is a composite material in which fibers are added to the fresh concrete mix [1, 2]. These fibers can improve the properties of the concrete in the fresh or hardened state. In structural applications, fibers can partially or totally replace the traditional reinforcement. For these purposes, the fibers provide an enhanced post-cracking tensile strength in the hardened state by bridging crack faces [3]. Commercially available fibers can be made from a number of different materials: steel, glass, synthetic and natural being the most common types [4]. Steel fibers are widely used in structural applications [5-8]. However, steel fiber reinforced concrete (SFRC) may not be suitable for all applications, and synthetic fiber reinforced concrete (SyFRC) [7] and glass FRC (GFRC) [9] have been successfully used as well.

While considerable research effort has been devoted to the material parameters and short-term structural characteristics of FRC [10-16], the long-term behavior of FRC elements is still poorly

understood [17-19]. One key element in long-term performance is creep, as time-dependent crack growth and crack widening may decrease durability. In particular, in cracked FRC elements, the fibers bridging crack faces are transmitting forces and as such, they are subjected to possible long-term loading. In the case of polymeric fibers, these sustained loads can give rise to creep deformations of individual fibers. In an FRC element, the fiber's own deformation can influence the crack width growth and therefore, it should be taken into account.

2. EXPERIMENTAL SETUP

2.1 Material characterization

In this research, two different polypropylene (PP) fibers are considered. These fibers are certified to be used in structural applications according to the European Standard EN 14889-2 [20]. Both types are commercially available in Belgium. Displacement controlled tensile tests were done to characterize the material, i.e. to determine the σ-ε curve. The test setup is shown in Figure 1(a). Uncut fibers, (3) in Figure 1(a), are clamped in a clamping setup, (2) in Figure 1(b), that uses a combination of gluing and clamping to minimize fiber end slippage. The displacement is measured by the internal gauge of the test machine, and an external load cell (capacity: 900 N, accuracy: ± 0.05 %) is used to record the applied force, see (1) in Figure 1(b).

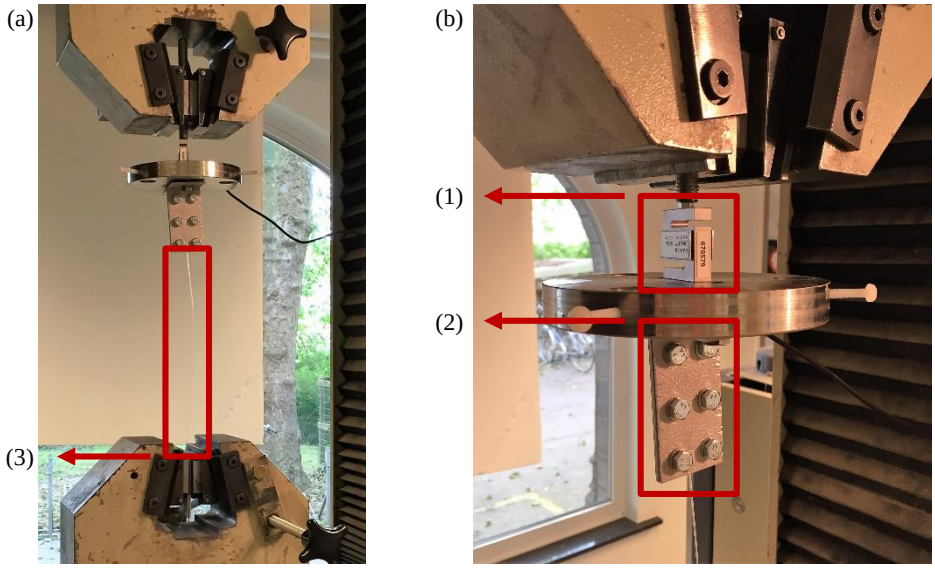

Figure 1 : (a) overview of the characterization setup (b) close-up of the load cell and clamping system with (1) load cell (2) clamping system (3) fiber

The tests characteristics are shown in Table 1. Fiber type A has been tested according to the European standard EN 14889-2 [20], while type B has been tested in accordance with the (yet unpublished) revision proposal of that standard. The data acquisition rate was 10 Hz for both fiber types.

Table 1: test characteristics for both fibers

	testing speed	initial fiber length	number of samples
type A	10 mm/min	430 mm	6
type B	50 %/min	250 mm	5

2.2 Creep frame

After the characterization of the fibers, both types are subjected to creep tests in a climate chamber at constant temperature (20 °C) and relative humidity (60 %). Uncut fibers were clamped on both sides using the same clamping system as used in the characterization tests. The fiber is then placed in a creep frame, and subjected to a sustained load until failure. The time-dependent fiber elongation is contactlessly measured by a laser sensor at a rate of 1 Hz in the first week, and at 0.1 Hz afterwards. The maximum measurable elongation is 125 mm. The creep setup is schematically shown in Figure 2 (a) and a photo of the actual frame is presented in Figure 2 (b).

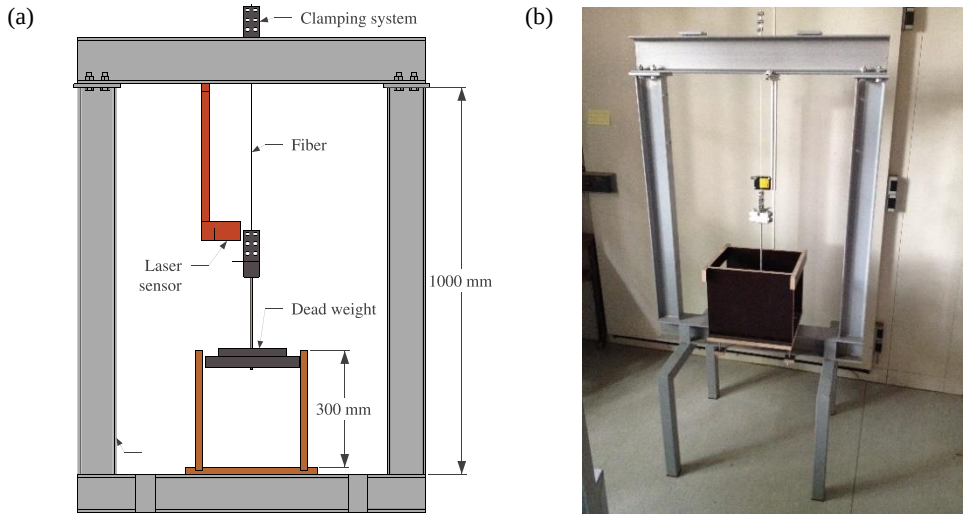

Figure 2: (a) simplified creep frame, not shown is the supporting base (b) photo of the creep frame

2.3 Creep specimens

In total, 26 creep samples have been tested, 14 of fiber A and 12 of fiber B. Every sample had an initial length of 200 mm and 5 different load levels were considered: 22 %, 36 %, 43 %, 53 % and 63 %. The load level is defined as the applied creep load with respect to the average tensile strength. The number of specimens per load level and fiber type are summarized in Table 2.

Table 2: number of creep specimens per load level and fiber type

load level	type A	type B
22 %	0	2
36 %	4	2
43 %	4	2
53 %	6	2
63 %	0	4
total	14	12

3. RESULTS

3.1 Material characterization

The σ-ε curves for type A and B are shown in Figure 3 (a) and (b), respectively. Furthermore, the fiber properties can be found in Table 3. The Young's modulus is calculated according to the revision proposal of EN 14899-2.

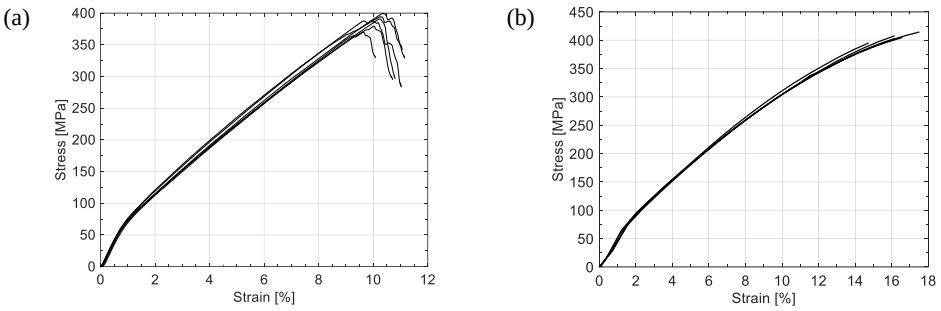

Figure 3: σ-ε curve for (a) type A and (b) type B

Table 3: mechanical properties of both fibers

	type A	type B
average strength (CoV†)	386.9 MPa (2.8 %)	404.7 MPa (1.8 %)
average strain at maximum stress (CoV)	10 % (2.6 %)	16.2 % (6.2 %)
average Young's modulus (CoV)	6205 MPa (2.7 %)	4529 MPa (1.5 %)

† CoV: coefficient of variation, ratio of the standard deviation w.r.t. the mean

3.2 Creep deformations

The creep results of fiber type A and B are shown on a logarithmic time scale in Figure 4 (a) and (b), respectively. In these figures × and * denote fiber creep failure, the former representing failure in the middle of the fiber, the latter failure near the clamps. ○ denotes an aborted test due to time constraints.

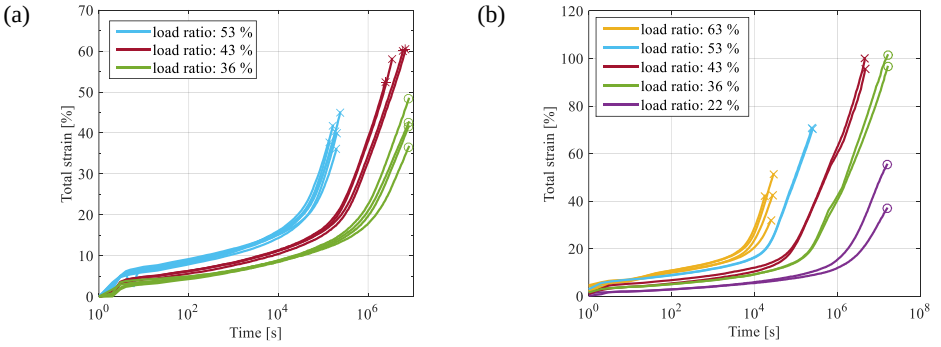

Figure 4: creep results of fiber type (a) A and (b) B.

The average time to failure and strain at failure, $t_{failure}$ and $\varepsilon_{failure}$ respectively, are summarized in Table 4a and Table 4b.

Table 4a: creep results of fiber type A

load ratio	$t_{failure}$ (CoV)	$\varepsilon_{failure}$ (CoV)
36 %	> 8.1×10^6 s (-)	> 43 % (11 %)
43 %	4.1×10^6 s (49 %)	58 % (6.3 %)
53 %	1.9×10^5 s (16 %)	40 % (7.8 %)

Table 4b: creep result of fiber type B

load ratio	$t_{failure}$ (CoV)	$\varepsilon_{failure}$ (CoV)
22 %	> 1.6×10^7 s (-)†	> 46 % (-)†
36 %	> 1.6×10^7 s (-)†	> 99 % (-)†
43 %	4.6×10^6 s (-)†	98 % (-)†
53 %	2.5×10^5 s (-)†	70 % (-)†
63 %	2.4×10^4 s (20 %)	42 % (19 %)

† CoV cannot be calculated for 2 specimens

It is clear that the load level significantly influences the time to failure as well as the total strain at failure. Overall, very large strains can be expected in relatively short periods of time: the time to failure ranges from several hours to several months for fibers loaded at 63 % or 43 % of their strength.

In all cases however, failure is sudden with no noticeable strain acceleration, that is usually associated with tertiary creep.

4. DISCUSSION

All fibers exhibited very large creep deformations. The relative creep deformation can be expressed in terms of a creep coefficient φ_{creep}. This is the ratio of the creep strain divided by the instantaneous strain, see Equation (1).

$$\varphi_{creep} = \frac{\varepsilon_{creep}}{\varepsilon_{instant}} \tag{1}$$

The average creep coefficient φ_{creep} is shown in Table 5. In general, large creep coefficients are observed, and these coefficients are strongly dependent on the load ratio with a decrease in load ratio corresponding to an increase in creep coefficient.

Table 5: average creep coefficient for all experiments (shown in parentheses is the CoV)

load level	type A	type B
22 %	N/A	> 14 (-)
36 %	> 15 (12 %)	> 15 (-)
43 %	16 (6.7 %)	12 (-)
53 %	8.8 (8.7 %)	7.7 (-)
63 %	N/A	4.4 (23 %)

With the results of type B, an estimation of the time to failure as well as the total strain at failure can be given for the fibers loaded at 36 % and 22 %. The extrapolation of both parameters is shown in Figure 5(a) and (b). Using these models, and assuming extrapolation is valid, it is possible to calculate the expected time to failure as well as the corresponding total strain at failure for the aborted tests, i.e. at a load ratio of 22 % and 36 %. The results are presented in Table 6.

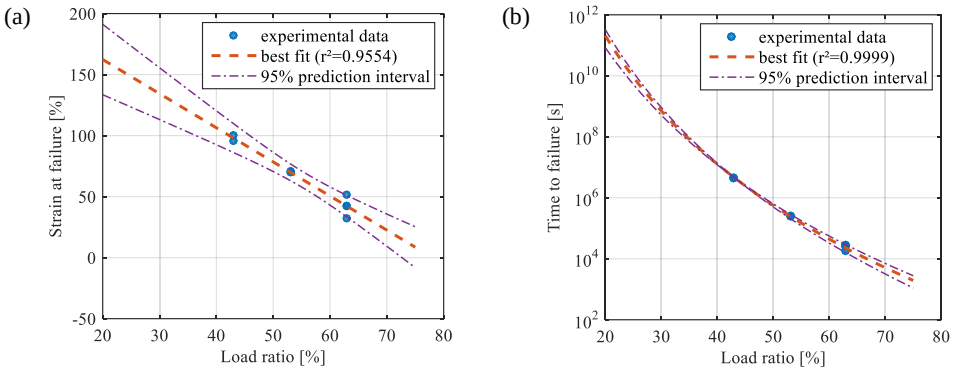

Figure 5: fiber type B extrapolation of the (a) strain at failure and (b) time to failure

Table 6: expected strain at failure and time to failure for the unfinished experiments

Load ratio	expected strain at failure (95 % confidence bounds)	expected time to failure (95 % confidence bounds)
22 %	157 %	5.4×10^{10} s
	(129 %, 184 %)	(2.6×10^{10} s, 8.3×10^{10} s)
36 %	118 %	5.5×10^{7} s
	(101 %, 134 %)	(4.7×10^{7} s, 6.3×10^{7} s)

There is good agreement between the fitted linear and power laws and the experimental data. These extrapolations underline the large expected creep strains. Furthermore, the results highlight the fact that the fiber's own creep strain can significantly widen a crack in an FRC element.

5. CONCLUSIONS

- Two types of commercially available structural polypropylene macrofibers have been subjected to sustained loading and the time-dependent deformations are recorded. All specimens had an initial length of 200 mm, and 5 different load levels were considered: 22 %, 36 %, 43 %, 53 % and 63 % of the average strength of the fiber.
- The strength of the fiber was determined according to the European standard EN 14889-2 for both fiber types in a displacement controlled test.
- In total, 26 creep specimens were tested. The results have shown that the load ratio strongly influences the time to failure as well as the total strain at failure. For one fiber type, an extrapolation with respect to these two parameters has been done in order to estimate the failure characteristics.
- No tertiary creep has been observed during the tests.
- The creep coefficient can be exceedingly large, and depends strongly on the load ratio.
- The results underline that the own fiber creep deformation can play an important role in the total crack width growth in FRC elements.

ACKNOWLEDGEMENTS

The author would like to thank the financial support of the Agency for Innovation by Science and Technology in Flanders (IWT).

REFERENCES

1. Balaguru, P. and S.P. Shah, *Fiber-Reinforced Cement Composites*. 1992, Texas, USA: Mcgraw-Hill.
2. Bentur, A. and S. Mindess, *Fibre Reinforced Cementitious Composites*. 1990, England: Elsevier Science Publishers LTD. 449.
3. di Prisco, M., G. Plizzari, and L. Vandewalle, *Fibre reinforced concrete: new design perspectives.* Materials and Structures, 2009. **42**(9): p. 1261-1281.
4. ACI Committee 544, *State-of-the-Art Report on Fiber Reinforced Concrete*, J.I. Daniel, Editor 2002, American Concrete Institute.
5. Serna, P., et al., *Structural cast-in-place SFRC: technology, control criteria and recent applications in spain.* Materials and Structures, 2009. **42**(9): p. 1233-1246.
6. Caratelli, A., et al., *Structural behaviour of precast tunnel segments in fiber reinforced concrete.* Tunnelling and Underground Space Technology, 2011. **26**(2): p. 284-291.
7. Bernard, E.S. *Design of Fibre Reinforced Shotcrete Linings with Macro-synthetic Fibres*. in *Shotcrete for Underground Support XI*. 2009.
8. de la Fuente, A., et al., *Experiences in Barcelona with the use of fibres in segmental linings.* Tunnelling and Underground Space Technology, 2012. **27**(1): p. 60-71.
9. Ferreira, J.P.J.G. and F.A.B. Branco, *The use of glass fiber-reinforced concrete as a structural material.* Experimental Techniques, 2007. **31**(3): p. 64-73.
10. *Fibre Reinforced Concrete*. RILEM Proceedings of the 5th RILEM Symposium (BEFIB 2000), PRO15, BEFIB 2000, ed. P. Rossi and G. Chanvillard. Bagneux, France: RILEM Publications S.A.R.L.
11. *Fibre-Reinforced Concrete*. RILEM Proceedings of the 6th RILEM Symposium (BEFIB 2004), PRO39, BEFIB 2004, ed. M. di Prisco, R. Felicetti, and G.A. Plizzari. Bagneux, France: RILEM Publications S.A.R.L.
12. *Fibre Reinforced Concrete: design and applications*. BEFIB 2008, ed. R. Gettu. Bagneux, France: Rilem Publication S.A.R.L.
13. Grzybowski, M. and S.P. Shah, *Shrinkage Cracking of Fiber Reinforced Concrete.* ACI Materials Journal, 1990. **87**(2): p. 138-148.
14. Pasini, F., et al., *Experimental study of the properties of flowable fiber reinforced concretes*, in *6th International RILEM Symposium on Fibre Reinforced Concretes*, M. di Prisco, R. Felicetti, and G.A. Plizzari, Editors. 2004, RILEM Publications SARL. p. 279 - 288.
15. Barros, J., et al., *Post-cracking behaviour of steel fibre reinforced concrete.* Materials and Structures, 2005. **38**(1): p. 47-56.
16. Buratti, N., C. Mazzotti, and M. Savoia, *Post-cracking behaviour of steel and macro-synthetic fibre-reinforced concretes.* Construction and Building Materials, 2011. **25**(5): p. 2713-2722.
17. Babafemi, A.J. and W.P. Boshoff, *Time-dependent behaviour of pre-cracked polypropylene fibre reinforced concrete (PFRC) under sustained loading.* Research and Applications in Structural Engineering, Mechanics and Computation, 2013: p. 1593-1598.
18. Babafemi, A.J. and W.P. Boshoff, *Tensile creep of macro-synthetic fibre reinforced concrete (MSFRC) under uni-axial tensile loading.* Cement and Concrete Composites, 2015. **55**(0): p. 62-69.
19. Zhao, G., M. di Prisco, and L. Vandewalle, *Experimental investigation on uniaxial tensile creep behavior of cracked steel fiber reinforced concrete.* Materials and Structures, 2014: p. 1-13.
20. CEN, *EN 14889-2: Fibres for concrete - Part 2: Polymer fibres - Definitions, specifications and conformity*, 2006, European Committee for Standardization.